A Wirelessly-Enabled, Power-Optimized, Low-Cost, and Open-Source Durafet-based pH Instrument for Continuous, Long Term Environmental Monitoring

Amelia L. Ritger
Ecology, Evolution, and Marine Biology
University of California, Santa Barbara
Santa Barbara, USA
aritger@ucsb.edu

David C. Burnett
Electrical and Computer Engineering
Portland State University
Portland, USA
dburnett@ece.pdx.edu

***Abstract*—The increasing acidity of our oceans, exacerbated by human activities, represents a growing threat to the human societies that rely upon healthy marine ecosystems. Research activities to collect data on the progression of ocean acidification are a crucial part of efforts to monitor, assess, and mitigate impacts. However, high-cost, commercially available monitoring tools represent a major barrier to comprehensive data collection and community engagement, especially for ocean acidification research. Here, we present an iteration to our open-source, low-cost pH sensor design which utilizes a Durafet pH electrode. We developed significant improvements to optimize energy consumption, simplify assembly, and add wireless functionality while maintaining affordability. We performed low-power hardware and firmware modifications which extend the battery lifespan. We designed a custom PCB that reduces assembly error, improves modularity, and maintains a compact footprint. Finally, we implemented bi-directional wireless functionality in our design, enabling wireless data retrieval and sensor re-programming, a feature that is notably absent in commercially available counterparts. With the addition of these features, we have designed open-source pH sensor electronics that are more affordable and accessible while maintaining high performance. Expanding sensor networks benefits everyone, by equipping researchers, policymakers, and communities with the knowledge and resources required to understand and adapt to our rapidly changing world.**

Keywords—Chemical sensors, environmental monitoring, oceanography, rapid prototyping, wireless communication

I. Introduction

As the world confronts the consequences of increasingly severe climate change events, there is a critical need for comprehensive environmental monitoring. Long term monitoring provides the foundation for researchers and policy makers to identify environmental baselines, develop predictive models, inform management strategies, and raise public awareness. Data gathering tools such as environmental sensors play a critical role in identifying, managing, and mitigating the impacts of a rapidly changing planet [1], [2]. However, the high cost of commercial instruments often creates barriers that hinder their widespread adoption, particularly by resource-limited research programs, which restricts our ability to comprehensively understand environmental changes at a global scale. These accessibility issues concentrate resources, bias research priorities, and impede broader engagement in research [3], [4], ultimately restricting our collective ability to effectively address the environmental challenges facing our world.

Some of these challenges are caused by ocean acidification, primarily driven by anthropogenic carbon dioxide emissions into the atmosphere. The reduction in ocean pH generates profound ecological transformations, posing major challenges for calcifying organisms [5], altering larval development in urchins [6], abalone [7], and fish [8], and disrupting food webs [9]. These effects extend to fisheries, further impacting social, economic, and cultural systems worldwide [10]. pH sensors are valuable tools for monitoring ocean acidification [11]–[13]; however, unlike other widely collected environmental parameters such as temperature and salinity, pH remains relatively understudied for long term monitoring partly due to the prohibitively high cost of commercially available sensors. This limitation results in a fragmented global ocean acidification monitoring network. Unfortunately, this information deficit disproportionately affects vulnerable coastal communities that rely on healthy marine ecosystems for recreational activities, cultural practices, and food security [10]. Geographically fragmented data leaves many communities and stakeholders without the information needed to effectively address local environmental challenges and develop adaptive resource management strategies.

Our work seeks to address this problem by developing a low-cost and open-source alternative to commercially available pH sensors, with a design that uses the industry-standard Honeywell Durafet pH electrode [14]. Our first design iteration focused on creating a simple, low-cost, compact datalogger that used an Arduino-based microcontroller to collect and store measurements from the Durafet [15]. Here, we present advancements that enhance the usability and performance of our previous design through the integration of wireless functionality and improved power management strategies. Both our previous iteration and the original design that inspired our project (used in [16]–[19]) requires users to remove sensitive sensor electronics from the waterproof housing to download data and re-program the sensor for calibration. Our design improvements extend the sensor's operational lifespan and reduce failure risk, making the design more versatile and robust for field deployments.

OCEANS 2024 - SINGAPORE | 979-8-3503-6207-7/24/$31.00 ©2024 IEEE | DOI: 10.1109/OCEANS51537.2024.10682142

II. Methods

Building upon our existing open-source pH sensor design [15], the modifications presented here introduce significant advancements to improve user experience and functionality. Our primary goals for this work were to:

- Keep component costs low to maintain affordability
- Improve power management to extend operating lifespan
- Integrate wireless functionality to enhance usability and reduce failure risk
- Design a dedicated PCB to reduce assembly complexity and signal crosstalk

A. Design

Our updated design uses an Adafruit Feather M0 Adalogger, Adafruit ADS1015 12-bit ADC, Adafruit ADS1115 16-bit ADC, DS3231 real-time clock (RTC), nRF24L01 transceiver, with a custom-designed PCB (Fig. 1). The Durafet pH electrode and associated temperature sensor signals are conditioned by a voltage divider before being passed through the ADCs (original design by [20], details in [15]). For our updated design, we transitioned the voltage divider from a protoboard with through-hole components to a dedicated PCB with surface mount components. The tolerances of the ceramic surface mount resistors and capacitors used on the PCB are ±0.1% and ±10%, respectively. The custom PCB also offers a predefined layout with clear markings for component placement (Fig. 2).

Our updated design also enables wireless communication, which is supported with an Arduino Pro Mini, nRF24L01 transceiver, and a CP2102 USB-to-UART module (Fig. 1). One 3V lithium coin cell battery supplies power to the RTC, and two 3.6V lithium batteries supply power to all other sensor components.

The materials cost for our updated design, excluding the Durafet and sensor housing, is presented in Table I. Documentation and instructions for building the new design iteration, including fabrication files for the custom PCB, are available on GitHub under the Apache 2.0 license: `https://github.com/ameliaritger/arduino-ph-sensor`.

B. Wireless communication

We enabled wireless communication with our sensor using nRF24L01 transceiver modules for bi-directional communication, paired with a normally-open reed switch that controls power supplied to the radio. The reed switch is triggered with a magnet, which sends an interrupt signal to power on the radio and initiate wireless communication between the Adalogger (receiver) and the Arduino Pro Mini (transmitter) plugged into a device (such as a laptop) via a CP2102 USB-to-UART module (Fig. 1). Power is supplied to the receiver for 30 seconds, during which time the receiver remains in a listening state awaiting a message from the transmitter.

To achieve remote programming and data retrieval, we implemented a wireless communication protocol [21] that

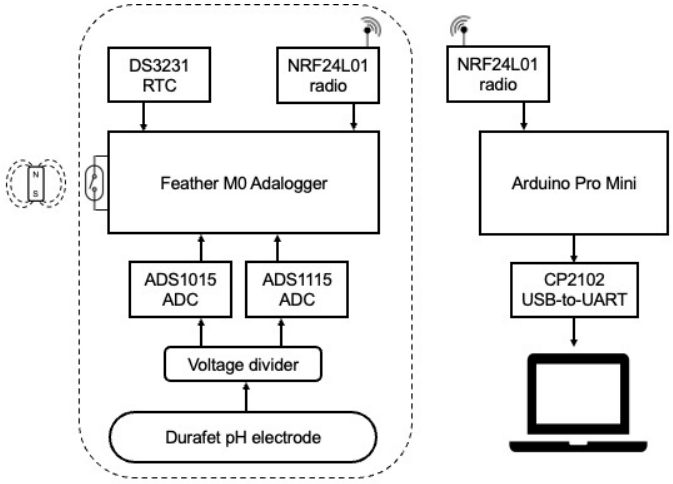

Fig. 1. Block diagram for electronic components. The outlined region denotes the sensor housing. An external magnet triggers the reed switch to initiate wireless communication. The computer icon signifies the device that communicates with the Arduino Pro Mini during wireless operations.

supports two message types: numeric messages, which transmit a numerical value to reprogram the sampling interval, and character messages, which instruct the sensor to transmit stored data back to the Pro Mini. Upon receiving a numeric message, the receiver overwrites the stored value for the sampling interval and then echoes the received message back to the transmitter, validating the programmed sampling interval. Upon receiving a character message, the receiver transitions to transmit mode and initiates file transfer if there is available data from the SD card. Data is read in 32-byte chunks from the file and transmitted sequentially, until the end of the file is reached and a final message is transmitted to indicate signal completion. If the transmitter sends a character message request when there is no new data to transmit, then the receiver module returns a negative acknowledgement message. After data transfer is complete, the receiver powers down and the sensor returns to sampling.

We tested wireless functionality indoors, with the receiver radio placed in the Schedule 80 PVC sensor housing and approx. 4 meters away from the transmitter radio. Our current wireless configuration uses a 250 kbps data rate, -12 dBm power amplifier level, and 16-bit cyclical redundancy checking length. These settings ensure data integrity and a higher resistance to noise, supporting wireless transmission distances sufficient for deployment applications. We also equipped both radio modules with additional 10 µF bypass capacitors to maintain stable power supply and mitigate transient voltage fluctuations during transceiver operation.

C. Low power modifications

We performed hardware and firmware modifications to our previous design to extend the operating lifespan of the device.

First, we utilized the DS3231 RTC interrupt pin to generate an alarm interrupt to wake up the Adalogger from sleep mode at a user-specified sampling interval. This maximizes the time the Adalogger spends in low power sleep mode when it is not actively collecting data. Next, we applied the DS3231 module low power modification developed in [22], including hardware

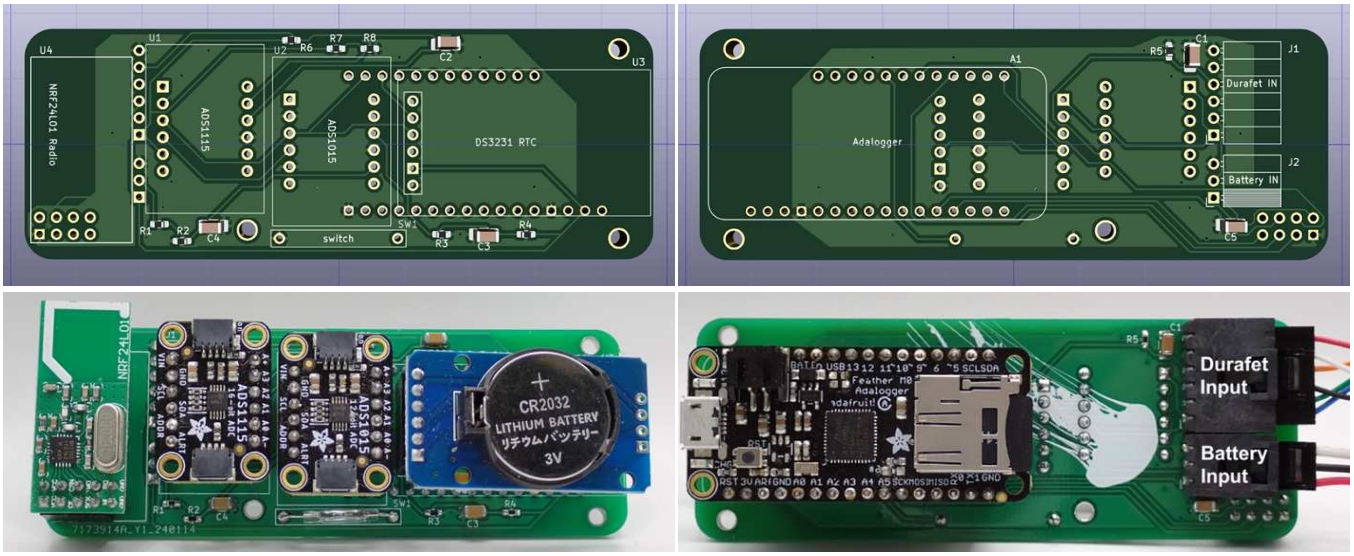

Fig. 2. Front (left) and back (right) of pH sensor electronics, displayed as a 3D model of the custom PCB (top) and photo of assembled components (bottom). Overall dimensions of the assembled electronics are approximately 95 x 25 x 29 mm (L x W x H).

and firmware alterations. These modifications enable the RTC to be powered entirely from the CR2302 coin cell backup battery (with a battery lifespan of approx. > 1 year in this configuration), removing its power draw from the system during sleep mode.

Additionally, we keep the nRF24L01 module powered down until it is triggered to wake up by magnetic activation of a reed switch. Upon activation by the reed switch interrupt, the receiver (Adalogger) remains in listening mode for 30 seconds before powering back down, unless there is a data transmission request from the transmitter (Arduino Pro Mini).

We also maximize the amount of time the ADCs spend in sleep mode when not converting measurements from the Durafet electrode by initializing the ADCs after an alarm interrupt, and then instructing the ADCs to return to sleep mode using the I2C general call reset. Likewise, due to the large current draw from the microSD card, we limit the amount of time the microSD card is interacted with by opening the file only after the ADCs are finished with measurement conversion.

Finally, we removed nonessential components estimated to consume at least 0.4 mA continuously. We removed one LED, the battery charger and its associated resistors from the Adalogger board. We also removed the power indicator LEDs from both ADC boards.

After performing these modifications, we measured current consumption using a Keysight E36312A Power Supply supplying ±3.6 V and a Keithley 2401 SMU set at a sampling rate of 5 samples per second. We used a custom Python script to interface with the instruments to capture and store current measurements in different operational states, including sampling, sleeping, and wireless transmission.

III. Results and Discussion

A. Design improvements

Our updated design incorporates a custom-designed PCB which acts as a platform for the Adalogger, voltage divider, and all other modules that comprise the internal sensor electronics (Fig. 2). Using a dedicated PCB optimizes component placement, reduces wiring complexity, and facilitates plug-and-play integration of modules. The modular design (1) utilizes silkscreen component outlines which simplify assembly through intuitive component placement, (2) enhances serviceability by enabling rapid identification and access to individual modules, and (3) promotes long-term reliability by reducing assembly errors. The use of surface mount components with tighter tolerances improves circuit performance while also supporting a more compact design. The current dimensions of the internal electronics are approx. 95 x 25 x 29 mm (L x W x H). For users willing to solder components onto the board, the custom PCB and passive components can be purchased for less than $40 (Table I). Importantly, our design's modularity facilitates future development and improvements, as additional components such

TABLE I. Current Costs for pH Instrument Electronics.

Item	Supplier	Cost (USD)
Feather M0 Adalogger	Adafruit	19.95
Arduino Pro Mini	Adafruit	11.95
ADS1015 ADC	Adafruit	9.95
ADS1115 ADC	Adafruit	14.95
DS3231 RTC module	Ebay	1.99
nRF24L01 radio module (x2)	Ebay	~2.00
CP2102 USB-to-UART module	Ebay	1.50
Custom PCB	JLCPCB	~7.00
Custom PCB components[a]	Digikey	~30.00
512 MB microSD card	Adafruit	4.95
3.6V AA lithium batteries (x2)	Digikey	8.00
3V CR2032 lithium battery	Ebay	~1.00
Total cost[b]		**$113**

[a.] Passive components such as resistors, capacitors, headers, and the reed switch.
[b.] Excludes fixed costs (e.g., the Durafet and PVC housing). Component costs were verified for accuracy at the time of manuscript submission.

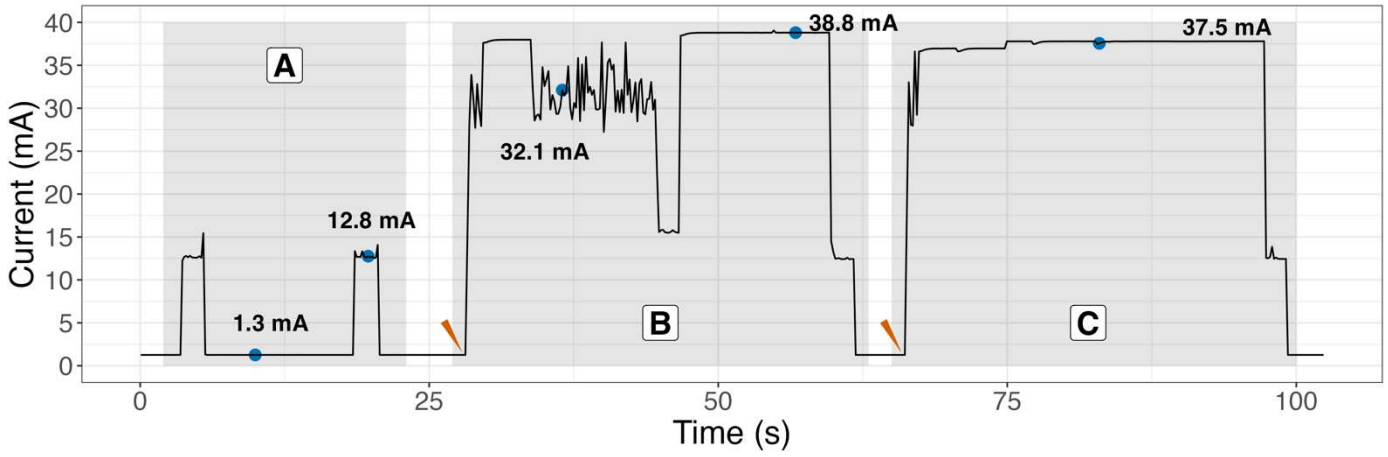

Fig. 3. Current consumption from the sensor while (A) sampling and sleeping, (B) after being woken up, wirelessly receiving instructions to send data, and then wirelessly transmitting data stored on the SD card before returning to listening mode, and (C) after being woken up, wirelessly receiving instructions to send data, and then wirelessly transmitting a message indicating there is no new data stored on the SD card before returning to listening mode. Time period (C) is also representative of current consumption when wirelessly receiving instructions to change sampling intervals. Blue points and associated current values illustrate representative data near the mean or maximum values for each period of interest. Red-orange triangles denote reed switch wakeup by a magnet.

as an external reference electrode or other sensors can be integrated into the board without extensive modification.

B. *Wireless communication*

With the addition of the nRF24L01 transceiver modules, Arduino Pro Mini and CP2102 USB-to-UART bridge and changes to firmware, we have upgraded our design to add wireless capabilities for around $15 USD (Table I). Our code enables wireless communication with the Adalogger through the Serial Monitor, allowing adjustments to the sampling interval and data retrieval from the SD card. With ongoing development, future iterations of the code may incorporate new features that expand the range of actions users may wirelessly perform.

Our wireless configuration sets the nRF24L01 to transmit 32-byte data packets every 10 ms. Each sampling point generates approx. 48 bytes of data; therefore, one month of data at a 15-minute sampling interval can be wirelessly downloaded via the Serial Monitor in approx. one minute, with a packet loss rate of less than 0.5%. The download time will fluctuate, however, depending on the connected device's specifications and network conditions.

While laboratory testing revealed a minor amount of data loss, it is likely attributable to the presence of interfering wireless signals indoors. We anticipate a reduction in data loss during field deployments due to the presence of fewer potential sources of interference. Regardless, given the inherent possibility of packet loss with the nRF24L01 transceiver, we recommend using wireless communication primarily for initial data quality checks, and prioritizing physical SD card retrieval to download data intended for analysis. A more advanced wireless mesh network system would transfer data more reliably and support many more wireless links than one single sensor, but at increased cost and complexity [23], [24].

The integration of wireless capabilities in our design expands the operational flexibility and data accessibility of the sensor, a feature that is notably absent in more expensive, commercially-available pH sensors. The current standard approach is to retrieve the sensors from the field periodically to download data and calibrate the electrode (if using Tris buffer) [25]. Unfortunately, traditional approaches require researchers to open the sensor housing and expose the internal electronics to potentially damaging environmental elements like moisture and contaminants. By enabling wireless communication in our updated design, we have eliminated this vulnerability by allowing researchers to change the sampling interval for *in situ* calibration and wirelessly download data for quality checks.

C. *Power requirements*

Although the hardware modifications to achieve lower power consumption require more upfront time during assembly, the resulting extension to deployment time outweighs the initial investment. At typical usage periods, the lifespan of the two 3.6V 2400 mAh lithium batteries in our design is estimated at 120 days, exceeding the longevity of our previous iteration [15].

When configured to oversample the temperature and pH signal from the pH electrode 64 times, a sampling event takes approx. 1.8 seconds to complete. During this time, the average current consumption is approx. 12.8 mA (Fig. 2a). In sleep mode, the average current consumption drops to approx. 1.3 mA (Fig. 2a). When the reed switch is triggered and the radio transceiver powers on, the average current consumption rises to approx. 32.4 mA in transmitting mode (Fig. 2b) and approx. 37.8 mA in listening mode (Fig. 2c). When the radio transceiver is powered down, its current draw is reduced to less than 1 µA.

D. *Considerations*

Our advancements represent a significant improvement over the first design iteration; however, trade-offs in power efficiency and some wireless features are inherent to our prioritization of a user-friendly, compact design.

First, while using an SD card for data storage offers undeniable advantages in accessibility, modularity, and scalability, it concurrently imposes a well-documented increase in power consumption (e.g., [26]–[28]). This is evident in our current iteration, where preliminary testing revealed a nearly 1

mA reduction in idle current after initialization without the SD card. However, targeted hardware and firmware modifications to the SD card module and surrounding circuitry may mitigate this drawback [22]. Despite their inherent power demands, SD cards remain the most readily available and user-friendly option for data storage and retrieval.

Next, the current operating lifespan of the sensor, powered by two lithium batteries, is approx. 120 days. Although extending the deployment time from months to years through additional batteries in parallel is technically feasible and a straightforward change to the modular design, it is not strictly necessary with the current application. Two main factors limit longer deployments: biofouling and sensor drift. First, prolonged exposure in the field significantly increases the risk of biofouling organisms growing on the electrode surface, significantly impacting data accuracy and necessitating regular cleaning and/or recalibration. Second, electrode readings can drift over time due to environmental factors and electrode aging. Sensor calibration, typically performed every 5-8 weeks, would also serve as opportunities to periodically monitor battery health. Therefore, although the batteries should not be at risk of draining during extensive deployments, the battery capacity can always be wirelessly checked during field visits to check for biofouling or perform sensor calibrations.

Finally, while the current wireless configuration supports a minimum transmission distance of 4 meters, an extended range and reduced packet loss could be achieved through integrating an antenna and adding a dedicated 3.3V power supply for the nRF24L01 transceiver. These changes would stabilize the signal and further offload the power demands from the lithium batteries powering the rest of the sensor electronics, extending the deployment timeframe for long-term monitoring. However, given the sensor's current usage and typical application range, the footprint increase due to the inclusion of an antenna outweighs the incremental performance gains, rendering it an unnecessary addition at this stage.

E. Areas for continued improvement

While we have successfully implemented several improvements with this design, there are still opportunities for further project development. Notably, there is significant potential for power optimization, as the current consumption of various components in sleep mode, while an improvement of our previous iteration, still exceeds datasheet specifications. For example, the implemented hardware and firmware modifications have resulted in the two ADCs consuming a combined approx. 0.3 mA while in sleep mode, which continues to exceed the stated 0.5 μA power down current for each device. Achieving this target would result in a substantial expansion of the operating lifespan of our device.

Cost and size reductions also offer avenues for future development. We can leverage the custom PCB and replace the modules with ICs to reduce costs, improve performance, and simplify maintenance with marginal increases in initial assembly effort. First, ICs are typically significantly cheaper than pre-assembled modules; for instance, the Texas Instruments ADS1115 chip costs roughly $6 compared to the $15 module offered by Adafruit. Second, purchasing ICs directly greatly reduces the risk of purchasing counterfeit chips, which is unfortunately common in the low-cost module marketplace. Third, using IC sockets maintains the modularity of using prefabricated modules, while reducing costs further during maintenance and repairs by only requiring the replacement of the individual chip rather than the entire module. As such, using individual ICs reduces the overall footprint of the internal electronics while also reducing electronic waste.

In addition, user experience can be improved by developing a dedicated graphical user interface (GUI). Currently, users need some familiarity with, or a willingness to navigate, the Arduino IDE. Although the code is functional and fully annotated, users who are less familiar with coding languages may find the IDE a less desirable interface for logger communication. A user-friendly GUI would simplify interaction and data retrieval, making the sensor more accessible to a broader audience.

Finally, looking beyond the immediate scope of this project, there is enormous potential for developing a low cost, high quality pH sensor by expanding improvements to the entire sensor system. Importantly, the Durafet pH electrode and its cap adapter currently comprise well over 50% of the entire cost of the sensor. Moreover, the electrode and its cap adapter take up a considerable footprint inside the sensor housing. We believe there are significant opportunities to reduce the footprint, in addition to the cost, through exploring alternatives to the Durafet pH electrode. The core functionality of this system could even be condensed into two pieces of silicon: one chip for processing and communication electronics and one chip for the sensor, as has been demonstrated with gas sensors [29]. Additionally, incorporating an external reference electrode holds potential for improving data accuracy and stability, and strengthens comparability with commercially available pH sensors. These efforts, along with planned additions such as a 3D-printable chassis to mount the electronics securely inside the housing, could yield a more compact, affordable, and user-friendly pH sensor in the tradition of existing rapidly-prototyped scientific instruments produced by and used for research [30], [31].

IV. Conclusion

We have improved our original pH sensor design by extending battery life, incorporating a custom-designed PCB, and enabling wireless communication in our system. These design updates represent a significant advancement in our goals to develop an affordable, accessible, and high quality pH sensor that can be built by anyone with access to basic electronics equipment. Notably, our integration of wireless communications to interface with the pH sensor during deployments is a feature that is absent in more expensive, commercially available counterparts. Our improvements extend the operating lifespan of the sensor, simplify assembly and troubleshooting, and mitigate the risk of damage to sensor electronics during data retrieval and *in situ* calibrations. Including wireless functionality and the custom PCB, the cost of the electronic components of our design is just over $100 USD.

We will continue development to make high performance, *in situ* pH sensors more affordable and accessible. We hope that our open-source design empowers more individuals to engage in environmental monitoring and stewardship, promoting equitable scientific participation and contributing to a deeper understanding of our changing planet.

ACKNOWLEDGMENTS

We would like to graciously thank F. Chan for his expertise and guidance on the original design of the pH sensor. We are grateful to K. Sam and D. Van Dalsem for their invaluable support with PCB design and KiCad. We thank A. Baish for their continued support of the project, including development of the custom Python script for test equipment interfacing to collect power measurements. We appreciate B. Hippe and T. Nguyen for their suggestions on system power optimization. We thank C. Nelson for taking their valuable time on land to procure a SeaFET for testing. We appreciate the words of encouragement by the members of the Hofmann lab. And we thank E. De Leon Sanchez, whose light box made our design shine for photos.

REFERENCES

[1] A. Tsatsaris *et al.*, "Geoinformation technologies in support of environmental hazards monitoring under climate change: An extensive review," *ISPRS Int. J. Geo-Information*, vol. 10, no. 2, 2021, doi: 10.3390/ijgi10020094.

[2] J. J. Lahoz-Monfort and M. J. L. Magrath, "A Comprehensive Overview of Technologies for Species and Habitat Monitoring and Conservation," *Bioscience*, vol. 71, no. 10, pp. 1038–1062, 2021, doi: 10.1093/biosci/biab073.

[3] B. Baker, "Frontiers of Citizen Science," *Bioscience*, vol. 66, no. 11, pp. 921–927, Nov. 2016, doi: 10.1093/biosci/biw120.

[4] Y. Katz and U. Matter, "On the Biomedical Elite: Inequality and Stasis in Scientific Knowledge Production," *SSRN Electron. J.*, vol. 7641, 2017, doi: 10.2139/ssrn.3000628.

[5] L. Mekkes *et al.*, "Pteropods make thinner shells in the upwelling region of the California Current Ecosystem," *Sci. Rep.*, vol. 11, no. 1731, pp. 1–11, 2021, doi: 10.1038/s41598-021-81131-9.

[6] P. C. Yu, P. G. Matson, T. R. Martz, and G. E. Hofmann, "The ocean acidification seascape and its relationship to the performance of calcifying marine invertebrates: Laboratory experiments on the development of urchin larvae framed by environmentally-relevant pCO2/pH," *J. Exp. Mar. Bio. Ecol.*, vol. 400, no. 1–2, pp. 288–295, 2011, doi: 10.1016/j.jembe.2011.02.016.

[7] R. N. Crim, J. M. Sunday, and C. D. G. Harley, "Elevated seawater CO2 concentrations impair larval development and reduce larval survival in endangered northern abalone (Haliotis kamtschatkana)," *J. Exp. Mar. Bio. Ecol.*, vol. 400, no. 1–2, pp. 272–277, 2011, doi: 10.1016/j.jembe.2011.02.002.

[8] C. Cattano, J. Claudet, P. Domenici, and M. Milazzo, "Living in a high CO2 world: a global meta-analysis shows multiple trait-mediated fish responses to ocean acidification," *Ecol. Monogr.*, vol. 88, no. 3, pp. 320–335, 2018, doi: 10.1002/ecm.1297.

[9] B. M. Jellison and B. Gaylord, "Shifts in seawater chemistry disrupt trophic links within a simple shoreline food web," *Oecologia*, vol. 190, no. 4, pp. 955–967, 2019, doi: 10.1007/s00442-019-04459-0.

[10] S. C. Doney, D. S. Busch, S. R. Cooley, and K. J. Kroeker, "The impacts of ocean acidification on marine ecosystems and reliant human communities," *Annu. Rev. Environ. Resour.*, vol. 45, pp. 83–112, 2020, doi: 10.1146/annurev-environ-012320-083019.

[11] L. Kapsenberg, S. Alliouane, F. Gazeau, L. Mousseau, and J. P. Gattuso, "Coastal ocean acidification and increasing total alkalinity in the northwestern Mediterranean Sea," *Ocean Sci.*, vol. 13, no. 3, pp. 411–426, 2017, doi: 10.5194/os-13-411-2017.

[12] G. E. Hofmann *et al.*, "Exploring local adaptation and the ocean acidification seascape - studies in the California Current Large Marine Ecosystem," *Biogeosciences*, vol. 11, no. 4, pp. 1053–1064, 2014, doi: 10.5194/bg-11-1053-2014.

[13] F. Chan *et al.*, "Persistent spatial structuring of coastal ocean acidification in the California Current System," *Sci. Rep.*, vol. 7, no. 1, pp. 1–7, 2017, doi: 10.1038/s41598-017-02777-y.

[14] T. R. Martz, J. G. Connery, and K. S. Johnson, "Testing the Honeywell Durafet® for seawater pH applications," *Limnol. Oceanogr. Methods*, vol. 8, no. MAY, pp. 172–184, 2010, doi: 10.4319/lom.2010.8.172.

[15] A. L. Ritger and D. C. Burnett, "Developing Low-Cost, Simplified, and Open-Source Durafet-based pH Instrument Electronics," *Ocean. 2023 - Limerick, Ocean. Limerick 2023*, pp. 1–7, 2023, doi: 10.1109/OCEANSLimerick52467.2023.10244512.

[16] M. H. Pespeni, F. Chan, B. A. Menge, and S. R. Palumbi, "Signs of adaptation to local pH conditions across an environmental mosaic in the california current ecosystem," *Integr. Comp. Biol.*, vol. 53, no. 5, pp. 857–870, 2013, doi: 10.1093/icb/ict094.

[17] K. J. Kroeker *et al.*, "Interacting environmental mosaics drive geographic variation in mussel performance and predation vulnerability," *Ecol. Lett.*, vol. 19, no. 7, pp. 771–779, 2016, doi: 10.1111/ele.12613.

[18] T. G. Evans, F. Chan, B. A. Menge, and G. E. Hofmann, "Transcriptomic responses to ocean acidification in larval sea urchins from a naturally variable pH environment," *Mol. Ecol.*, vol. 22, no. 6, pp. 1609–1625, 2013, doi: 10.1111/mec.12188.

[19] J. M. Rose *et al.*, "Biogeography of ocean acidification : Differential field performance of transplanted mussels to upwelling-driven variation in carbonate chemistry," pp. 1–25, 2020, doi: 10.1371/journal.pone.0234075.

[20] G. Freiderich, "Custom pH sensor voltage divider design for nearshore marine deployments." unpublished, Monterey Bay Aquarium Research Institute.

[21] Robin2, "Simple nRF24L01+ 2.4GHz transceiver demo," *Forum.arduino.cc*. https://forum.arduino.cc/t/simple-nrf24l01-2-4ghz-transceiver-demo/405123 (accessed Jan. 29, 2024).

[22] P. A. Beddows and E. K. Mallon, "Cave pearl data logger: A flexible arduino-based logging platform for long-term monitoring in harsh environments," *Sensors (Switzerland)*, vol. 18, no. 2, 2018, doi: 10.3390/s18020530.

[23] R. Leon *et al.*, "The Networked Nitrous Node: A Low-Power Field-Deployable COTS-Based N2O Gas Sensor Platform," *IEEE Sensors Lett.*, vol. 7, no. 6, 2023, doi: 10.1109/LSENS.2023.3276339.

[24] B. P. Hippe, A. A. Dezay, M. A. Garcia, M. C. Newton, J. M. Acken, and D. C. Burnett, "Multi-Node Networked Indoor Air Quality Monitor," *Proc. IEEE Sensors*, pp. 1–4, 2023, doi: 10.1109/SENSORS56945.2023.10324899.

[25] A. G. Dickson, "The measurement of sea water pH," *Mar. Chem.*, vol. 44, no. 2–4, pp. 131–142, 1993, doi: 10.1016/0304-4203(93)90198-W.

[26] L. Gough, "Experiment: microSD card power consumption & SPI performance," *Goughlui.com*. https://goughlui.com/2021/02/27/experiment-microsd-card-power-consumption-spi-performance/ (accessed Jan. 29, 2024).

[27] M. Gaidica, "Low Power Showdown: uSD Card Sleep and Write Current Draw," *Gaidi.ca*. https://gaidi.ca/weblog/low-power-showdown-usd-card-sleep-and-write-current-draw/ (accessed Jan. 29, 2024).

[28] E. Mallon, "Cutting Power to Secure Digital Media cards for Low Current Data Logging," *Thecavepearlproject.org*. https://thecavepearlproject.org/category/reducing-power-consumption/ (accessed Jan. 29, 2024).

[29] D. C. Burnett *et al.*, "Two-Chip Wireless H2S Gas Sensor System Requiring Zero Additional Electronic Components," *2019 20th Int. Conf. Solid-State Sensors, Actuators Microsystems Eurosensors XXXIII, TRANSDUCERS 2019 EUROSENSORS XXXIII*, pp. 1222–1225, 2019, doi: 10.1109/TRANSDUCERS.2019.8808294.

[30] D. C. Burnett, B. L. Smarr, S. M. Mesri, L. J. Kriegsfeld, and K. S. J. Pister, "Reconfigurable, wearable sensors to enable long-duration circadian biomedical studies," *BODYNETS 2014 - 9th Int. Conf. Body Area Networks*, vol. 1, pp. 142–146, 2014, doi: 10.4108/icst.bodynets.2014.257078.

[31] B. L. Smarr, D. C. Burnett, S. M. Mesri, K. S. J. Pister, and L. J. Kriegsfeld, "A Wearable Sensor System with Circadian Rhythm Stability Estimation for Prototyping Biomedical Studies," *IEEE Trans. Affect. Comput.*, vol. 7, no. 3, pp. 220–230, 2016, doi: 10.1109/TAFFC.2015.2511762.